Microsyst Technol (2011) 17:403–409
DOI 10.1007/s00542-010-1199-1

TECHNICAL PAPER

A polymer-based bidirectional micropump driven by a PZT bimorph

Yi Luo · Miao Lu · Tianhong Cui

Received: 24 September 2010 / Accepted: 20 December 2010 / Published online: 4 January 2011

Abstract This paper presents a polymer-based micropump for liquid control or drug delivery. The dimension of the pump was 20 × 24 × 3 mm^3. A pair of O-ring SU-8 passive valves was fabricated by lift-off technique to control the fluid movement. Micropumps with dimple, bridge, and cantilever valves were studied. The PZT bimorph acted on the polymer membrane to periodically drive fluid. The maximum flow rate was 16.4 ml/min, and the back pressure was 1,525 mmH_2O at 150 V (Vp-p). In frequency sweeping experiments, two flow rate peaks and back pressure peaks were analyzed. Bidirectional flow rate was achieved by changing the valve seat from a one-size hole to a step hole. The maximum backward flow rate was 5.1 ml/min, and the driving frequency was about 355 Hz higher than the forward flow rate driving frequency.

1 Introduction

Microelectromechanical system (MEMS) enabled a wide range of miniature actuators and sensors. Since the early years of MEMS development, micropumps were among the early generation devices in micro scale, and fabricated with microfabrication technologies. With the growing importance of the miniaturization of microfluidic systems, the micropump is becoming an very active research topic. Controlling or dispensing the liquid in body has been a long-term goal of micropump designer. However, most of the existing micropumps were fabricated by silicon or glass (Koch et al. 1997; Hwang et al. 2007; Yoon et al. 2007; Doll et al. 2007). The Young's modulus of the silicon or glass is much higher than polymer, resulting in higher driving voltages in pumping operation, causing potential insulation problems. The silicon micropump is not a good choice to be embedded into human bodies for its fragile and non-biological compatibility.

In recent years, polymer MEMS devices have shown their low cost, good biocompatibility and good chemical resistance in microfluidic systems. One promising trend is to design polymeric micropumps. Pumps fabricated by micro injection molding and laser technique (Gietzelt et al. 2002; Kamper et al. 1998), hot embossing (Han et al. 2003), and micro machining (Bohm et al. 1999) were reported. Reliability and power consumption are critical for implantable micropumps. Overpressure at the outlet of the valveless diffusion pumps will cause backflow, and will become predominant when the pump is switched off, while the micropump with check valves can prevent unintended (Chen et al. 2008). Moreover, the pumps with check valves have bubble-tolerance characteristics if the volume stroke ratio is large enough. Usually, the valves can be categorized as either active or passive. Active valves are operated by actuation force and offer improved performance, however, increase complexity and fabrication cost. Passive valves do not include any actuation (Nisar et al. 2008). The pressure exerted on the working fluid through the movable membranes, the passive valves at the inlet and outlet are oriented to favor flow into and out of the pump chamber by the pressure difference. Optimizing the structure of micropump and driving condition can make passive valve pump working more efficiently. Meanwhile, bidirectional also can realize on a passive valved micropump (Zengerle

Y. Luo and M. Lu contributed equally to this work.

Y. Luo · M. Lu · T. Cui (✉)
Department of Mechanical Engineering,
University of Minnesota, 111 Church Street S. E.,
Minneapolis, MN 55455, USA
e-mail: tcui@me.umn.edu

et al. 1995), and this has been a new challenge to broaden the application range of the microfluidic devices. Among the various types of working principles, the micropump using membrane actuation is known as a promising approach. Micropumps usually employed piezoelectric actuation (Gietzelt et al. 2002; Zengerle et al. 1995; Truong et al. 2004), electromagnetic actuation (Lee et al. 2008; Shen et al. 2008), and thermopneumatic actuation (Wego et al. 2001; Cooney et al. 2004) as their actuators. Electromagnetic actuation method need introduce extra magnetic field. Overheating in thermopneumatic actuators can result in the deterioration of biomaterials. On the contrary, piezoelectric actuation is known as an efficient liquid pumping approach because it has many advantages including sub-nanometer resolution, high mechanical force, absence of magnetic fields, no mechanical wear, and compatibility with clean, vacuum environments. Furthermore, due to the increasing needs in biochemical field for a high throughput, piezoelectric actuated micropump is easy to reliably control liquids in a microliter range. However, piezoelectric actuation also exist some problems, such as high input voltages and relatively small stroke volumes (Lee et al. 2006).

In this study, a series of polymer-based micropump were designed, fabricated, and characterized, aiming at operating under a relatively low driving voltage suitable for human bodies. Since it is fully polymeric, this pump can be made in a simple design and fabrication, which is helpful for miniaturization and compatible to polymer MEMS fabrication. Meanwhile, the Young's modulus of the valve and membrane is smaller than rigid materials, which can promote the stroke volume, helping the pump to work under a lower driving voltage. Different valve styles were studied to analyze the pump performance, and step-hole valve seat was fabricated to get the bidirectional flow rates. A PZT bimorph was used as the actuator, the performance characteristics were investigated by experiments to find the optimized operating conditions and to further optimize the geometry and performance of the micropump.

2 Micropump design and fabrication

The micropump consists of three units: inlet/outlet unit, valve unit, and vibration unit. These three units were bonded by epoxy glue, as shown in Fig. 1. The inlet/outlet unit was assembled by an inlet pipe and an outlet pipe (Tygon, USA) and a polymethyl methacrylate (PMMA) substrate. The diameter of the inlet and the outlet pipe was the same. The inner and outside diameters were 1.6 and 3.2 mm, respectively. Two holes were drilled on the PMMA substrate with the diameter of 3.2 mm to assemble inlet and outlet pipes.

The valve unit was assembled by three layers: upper PMMA valve seat, O-ring SU-8 valve, and lower PMMA valve seat. The dimension of both upper and lower PMMA valve seat was 12×20 mm^2, and the thickness was 0.75 mm. The diameters of holes on the upper and lower valve seat were 1.2 and 5 mm, respectively. The three valves are shown in Fig. 2. On the SU-8 valve base, there was an SU-8 O-ring to help sealing to the small hole on the upper PMMA substrate in the vibration. The three layers were bonded by glue. There were two valve units in one pump, as shown in Fig. 1b. One unit was served as the inlet, and the other unit was served as the outlet.

The O-ring SU-8 valve was fabricated by lift-off technique. Figure 3 depicts the schematic of fabrication process. The process started with spin coating LOR 3A (Microchem Corp., USA) on the silicon wafer as a sacrificial layer. The spin coating speed was 3,000 rpm and soft

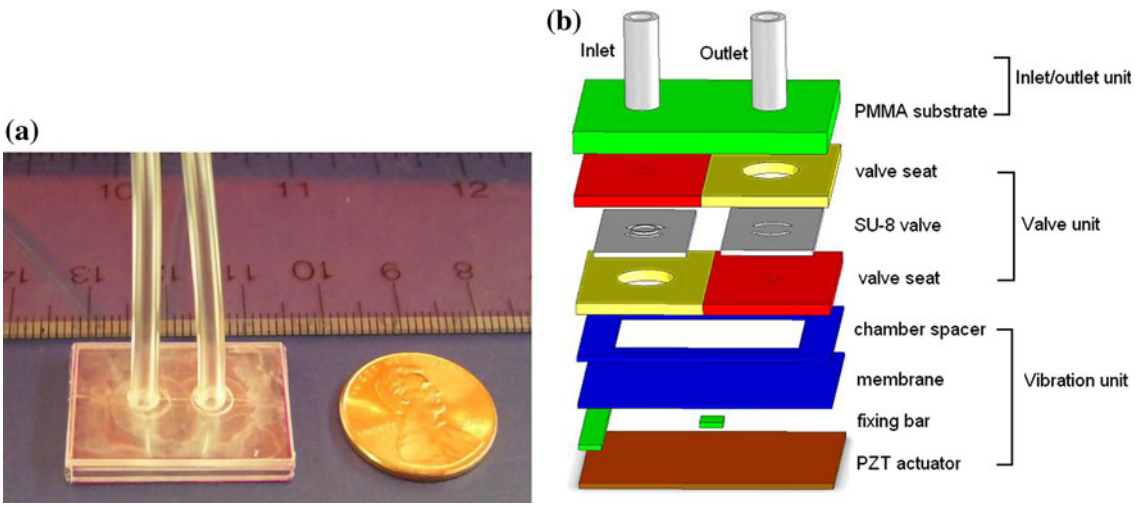

Fig. 1 Flexible polymer-based micropump. **a** The assembled micropump, **b** schematic of micropump

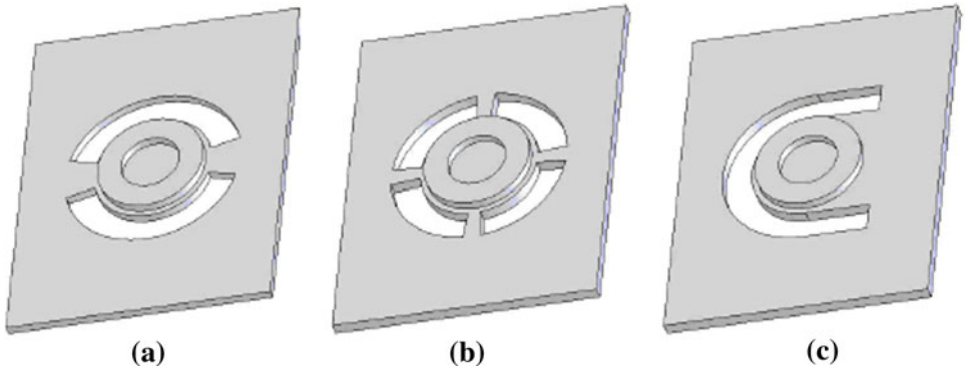

Fig. 2 Valve style. **a** The dimple valve, **b** the bridge valve, **c** the cantilever valve

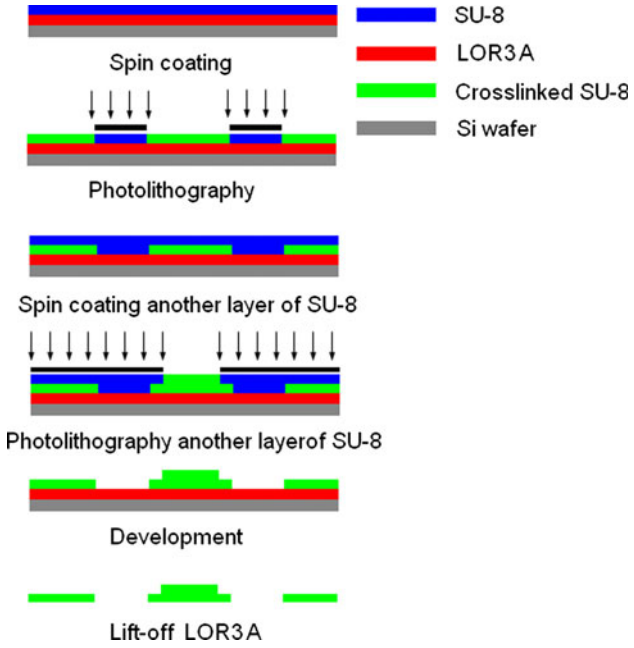

Fig. 3 Schematic of the fabrication process of SU-8 check valve

baked at 150°C for 3 min. Next, SU-8 3050 photoresist (Microchem Corp., USA) was spin coated on it. After a two-step soft baking, 65°C for 10 min and 90°C for 40 min, the wafer was exposed under the UV light for 1 min, using the dimple pattern mask. The thickness of the SU-8 depends on the spin coating speed. In this paper, the spin coating speed of 2,250 rpm resulted in the valve thickness of 60 μm.

The O-ring was fabricated by another layer of SU-8. To strengthen the bonding force between the two SU-8 layers, the post exposure baking (PEB) and development of the first SU-8 lithography process was diminished. Another layer of SU-8 spin coated directly at a speed of 2,500 rpm to build an O-ring with the thickness of 50 μm. Two-step soft baking took place at 65°C for 10 min and 85°C for 50 min to ensure the first layer of SU-8 cross-linked and the second layer's solvent evaporated thoroughly. Using the O-ring pattern mask, the wafer was exposed under the UV light for 1 min. Two-step PEB took place at 65°C for 10 min, followed by backing at 85°C for 40 min. After cooled down to the room temperature and relaxed for 60 min, the wafer was developed in propylene glycol methyl ether (PGMEA) for about 6–7 min. The wafer was rinsed by isopropyl alcohol (IPA), and put into MF™ CD-26 (Rohm and Haas Electronic Materials, USA) to lift off the LOR 3A for 16 h. Finally, after rinsed with DI water, the O-ring SU-8 check valves were fabricated.

The vibration unit was assembled by polymer film membrane (3 M PP2500 transparency film) and PZT bimorph (Kunshan Jingfeng Electronics). The polymer membrane film was glued to the valve unit by a same material spacer 0.1 mm thick to build a chamber. The depth of the chamber was 0.1–0.15 mm, generated by the thickness of the glue and film. The dimension of bimorph PZT actuator was 20 × 24 mm^2. It was a brass plate with PZT on both sides, and the total thickness of the PZT actuator was 0.59 mm. The thickness of brass and one layer of PZT were 0.09 and 0.25 mm, respectively. The d_{31} of PZT was −575 pC/N. Cantilever and peripheral fixed boundary condition of PZT were studied, and experiments showed that the cantilever driving boundary condition was better than the peripheral fixed. The displacement of cantilever boundary condition of PZT was larger than the peripheral fixed boundary condition, while the resonance frequency was lower, which matched the SU-8 valve vibrated in water. The length of the cantilever was 12 mm. The actuating boundary condition was shown in Fig. 1b.

According to structure mechanism and piezoelectric theory, ignored the influence of brass layer because it is very thin, the displacement and force generated by a cantilever PZT actuator can be calculated in the following equation:

$$\Delta x = \frac{3}{4} d_{31} \left(\frac{l}{t}\right)^2 V \tag{1}$$

$$F = \frac{3}{2} Y w d_{31} \left(\frac{t}{l}\right) V \tag{2}$$

where Δx is the displacement at DC voltage, F is the generated force, d_{31} is the piezoelectric coefficient in the "1" direction, l, t, w are the length, thickness, and width of PZT film, respectively, V is the applied voltage, and Y is the Young's modulus of PZT. The displacement and force generated by the PZT actuator under the effective values of the voltage of 50 V are 49.7 μm and 0.61 N, respectively.

The hydraulic pressure is $p = \frac{F}{S}$, where S is the area of the chamber. According to the F calculated above, the hydraulic pressure is 1.54 kPa. The inlet resistance is 100 mmH_2O from the experiments, indicating that when the hydraulic pressure is larger than 0.98 kPa, the valve can be opened. The preliminary estimation proved that the cantilever boundary condition of PZT bimorph can satisfied the pump actuation.

3 Experiments and discussion

The testing apparatus consisted of a beaker, a signal generator, an oscilloscope, and the micropump. The beaker was a water source, the signal generator generated square wave signal. The oscilloscope detected the wave style and voltage on the PZT. The working liquid of the pump was water. Three micropumps were assembled. They were basically the same, except that the SU-8 O-ring valves were different.

The flow rate at different driving frequency and voltage (Vp-p) is shown in Fig. 4. The maximum flow rate of three pumps at 150 Vp-p were 15 ml/min for dimple valve pump, 16.4 ml/min for bridge valve pump, and 8.4 ml/min for cantilever valve pump, respectively.

Both driving frequency and voltage influenced the flow rate of micropumps. In general, the flow rate increased with the driving frequency and voltage. Since the PZT vibration displacement increases with the voltage, the stroke volume of each cycle increased consequently. The volume of the pump chamber was a constant value, thus the dead volume would be decreased, resulted in the increasing of the compression ratio, thus the pump can drive more water into the outlet in each cycle, and finally lead to the increase of the flow rate. The pump also had a threshold voltage value to work, which means below that voltage, the pump cannot overcome the resistance to work. To overcome the inlet resistance of about 100 mmH_2O, the voltage should be over 64 Vp-p for a square wave.

Dimple valve pump has one peak flow rate, with bridge valve pump and cantilever valve pump have two peaks. The first flow rate peaks for three micropumps are 775 Hz for dimple valve pump, 775 Hz for bridge valve pump, and 750 Hz for cantilever valve pump respectively. This means that the resonance frequency of bimorph PZT actuator and the mass of the entire pump influence the resonance frequency of the pump, while the valve style has little influence on the first flow rate peak. The resonance frequency of the valve vibrated in water also influences the flow rate. When swept the driving frequencies, two styles of valves, bridge style and cantilever style, had two peaks. The second peak was the resonance frequency of a valve in water. They were 875 Hz for bridge valve and 1,075 Hz for cantilever valve. The resonance frequency of valve in water influenced its opening distance. At the valve resonance frequency, though the PZT actuator cannot reach the highest amplitude, the resistance of water flow can be reduced, and this helps to get a high flow rate. For bridge style valve pump, the two frequencies of two flow rate peaks were closed, with a difference of 100 Hz, therefore the second peak had a higher flow rate, for the valve vibration reinforces the flow rate, while the PZT vibrates at relatively large amplitude. For the cantilever pump, the gap of the two peaks was 300 Hz. The cantilever valve is softer than the other two valves. The first order resonance

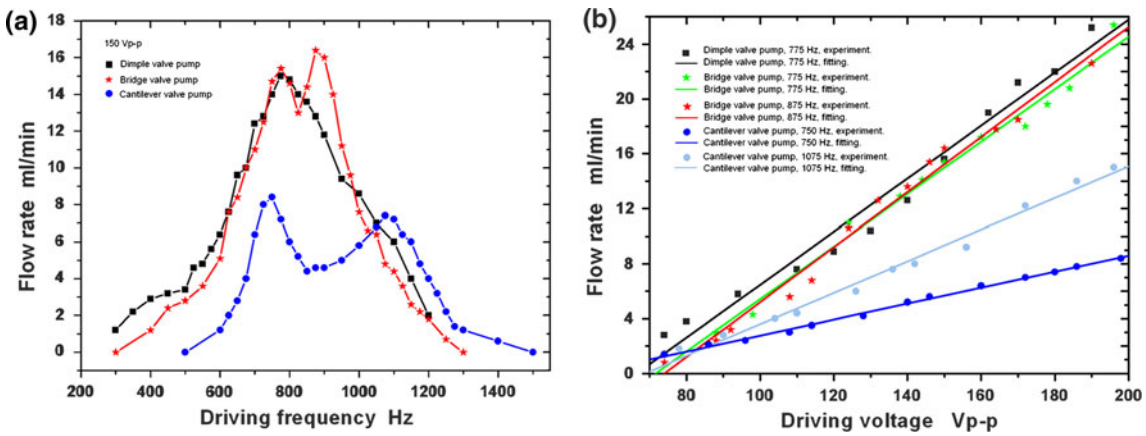

Fig. 4 The flow rate behavior of the micropump. **a** Flow rate with the change of driving frequency, **b** flow rate with the change of driving voltage

frequency of the cantilever valve in water was 200 Hz, while the first order resonant frequency of pumping membrane driven by PZT was 1,075 Hz. The amplitude of the PZT vibration was much smaller than the valve displacement. Therefore, the second flow rate peak was lower than the first one. The dimple style valve pump did not have two peaks, however, the peak of its flow rate was wider.

The valve style also influences the flow rate. Compared to the dimple and bridge style, the cantilever valve micropump had the smallest flow rate at the same driving voltage. The reason is that the cantilever valve was the softest, and the resonance frequency of PZT and mass of the pump did not match the valve vibration in water.

The back pressure at different driving frequency and voltage (Vp-p) is shown in Fig. 5. The highest back pressures were at 775 Hz for a dimple pump, 830 Hz for a bridge pump, and 1,100 Hz for a cantilever pump, respectively. The bridge style pump did not have two back pressure peaks. Instead, the peak of back pressure appeared at 830 Hz, almost at the center of 775–875 Hz for the two flow rate peaks. For the cantilever valve pump, there were two peaks, 750 and 1,100 Hz, fitted the flow rate peaks with a deviation of only 25 Hz. Increasing the driving voltage at a certain frequency can increase the back pressure, the relationship between driving voltage and back pressure was almost linear, as shown in Fig. 5b. Different valve need a different driving voltage to get the same back pressure. For dimple valve micropump, the back pressure at 104 Vp-p was 1,300 mmH_2O. For bridge valve micropump, the voltage raised to 145 and 135 V for the cantilever valve pump. The high flow rate of a micropump did not mean a high back pressure. Because the back pressure relies not only on the water pumping out, but also on the valve sealing to the small-hole valve seat, especially for a high back pressure circumstance.

The response of back pressure was measured with the pressure transducer DPT100 (Utah Medical Products, Inc., USA). The recording set-up consists of an iWorx404 interface connected to an ETH-255 Bridge/Bio Amplifier (iWorx/CB Science Inc., USA). The pump response curve was shown in Fig. 6. It took 0.09 s to change the back pressure from 41 to 392 mmH_2O. For a high back pressure, it took 1.05 s to change the back pressure from 440 to 802 mmH_2O. The later change included the time of increase the voltage manually. The experiment shown that the response time of the micropump is very fast.

4 Bidirectional pump

According to the experiments of two flow rate peaks, the membrane vibration was not synchronous with the valve vibration in water. The phase shift between them had a potential to change the direction of a flow from forward to backward. A new structure in chamber was designed to add the phase shift, and finally realized bidirectional flow. The detailed structure in chamber is shown in Fig. 7. The PMMA substrate had a step hole, and the diameter of the large one is 5 mm, the same as the large-hole valve seat in the valve unit. The diameter of the small one was 3.1 mm. The total thickness of the substrate was 0.75 mm, while the thickness was 0.3 mm. The thickness of the chamber was 0.18 mm.

For bridge valved micropump, the flow rate versus driving frequency at a 150 Vp-p square wave is shown in Fig. 8. The maximum forward flow rate was 6 ml/min at 620 Hz, while the maximum backward flow rate was 5.1 ml/min at 975 Hz. The forward flow rate peak was smaller than the original pumps, since the total mass of the pump was increased by a larger chamber.

It is possible to realize a bidirectional micropump with passive valves. According to the reference (Zengerle et al.

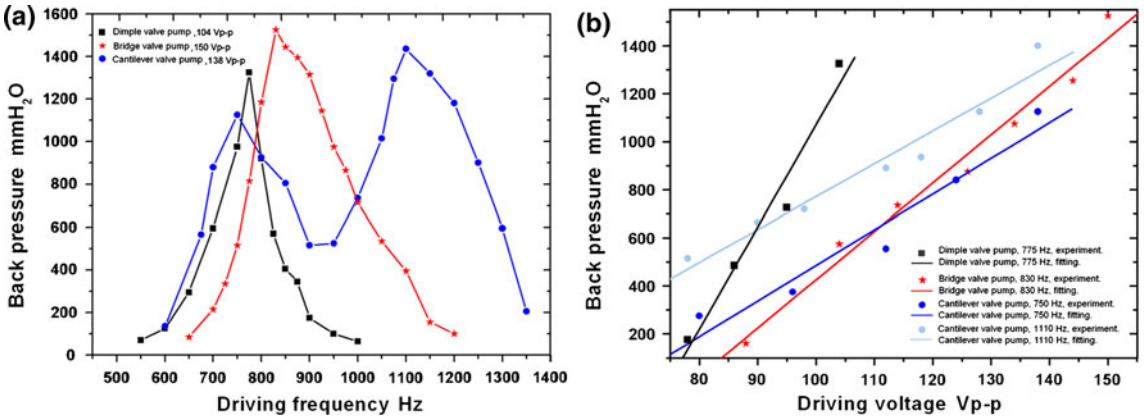

Fig. 5 The back pressure of the micropump. **a** Back pressure with the change of driving frequency, **b** back pressure with the change of driving voltage

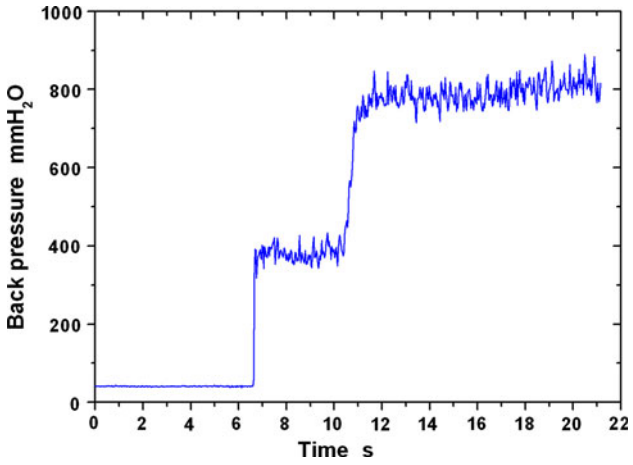

Fig. 6 The response behavior of back pressure of the micropump

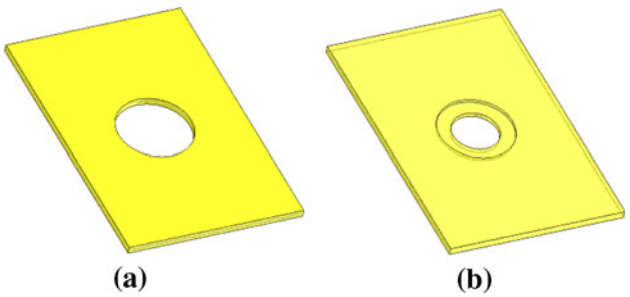

Fig. 7 PMMA large hole valve seat. **a** The original valve seat, **b** step hole valve seat

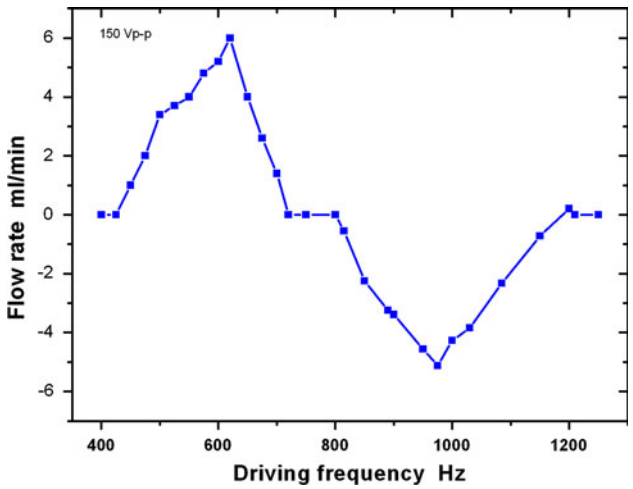

Fig. 8 The forward and backward flow rate of the micropump

1995), the fluid flow through the valve depends on two parameters: (i) the displacement of the valve opening; (ii) the hydrostatic pressure difference drives the fluid through the gap of the valve opening. They are not always working synchronously, which approved by the experiments in Sect. 3.1 by two peaks flow rate. When the driving frequency is equal to or higher than the resonance frequency of valve in water, there is a phase shift between the driving pressure and the valve movement. The performance of the pump will change when the driving frequency from lower than resonance frequency of valve to higher than that resonance frequency. When the driving frequency is higher than the resonance frequency, the movement of passive valve is behind the pressure signal, which drives the fluid as well as the valve. Thus the pressure signal is partially directed the backward direction, while the valve is still open in the forward direction. As a result of this, the backward direction flow will cancel part of the flow in the forward direction. When the driving frequency keeps higher, the phase shifts more and the backward flow exceeds the forward flow rate, the micropump appears the backward flow rate. In this paper, the backward flow rate peak occurred at a frequency of 975 Hz, 100 Hz higher than the resonance frequency of valve vibration in water.

The micropump structure also helps to realize a bidirectional flow. The small hole on the substrate disturbs the hydraulic pressure generated by the membrane in the chamber, making the valve easier to vibrate at its resonance frequency in water. This makes the backward flow rate more distinctive. An increase of the chamber depth also helps to reduce the frequency influence of the vibration source to the valve. Both the forward and backward flow rates are smaller than the original bridge valve micropump, for the compression ratio of this pump was decreased with the increase of chamber thickness. Bidirectional micropump is useful in a liquid control system or drug delivery in human bodies, reducing two pumps to one for bidirectional liquid control.

5 Conclusions

A series of polymer-based micropumps were designed, fabricated, and characterized in this work. They were actuated by a PZT bimorph. The materials are cheap, and manufacture process is simple, which make the micropump disposable, diminishing the cross contaminations of chemicals. Since the polymer has a lower Young's modulus and its thickness is easy to change by spin coating and other MEMS fabrication methods, the polymer-based pump can work under a relatively low driving voltage. The lowest driving voltage was 64 Vp-p. The driving voltage can be further reduced for implantable devices, and it can simplify the problem of electric insulation and reduce the power consumption. The maximum flow rate under 150 Vp-p square wave was 16.4 ml/min, the highest back pressure was 1,525 mmH_2O. Bidirectional flow rate was realized on the step-hole valve seat micropump. Backward flow rate was achieved at a higher driving frequency due to the phase shift caused by different driving frequency of

PZT actuator and resonance frequency of valve. The maximum backward flow rate was 5.1 ml/min at 150 Vp-p.

In the future, the bidirectional polymeric micropump may become the key component of micro fluidic systems, such as micro purge system, electro-mechanical occlusive devices, micro mixer, etc. Future work will be focused on the bidirectional driving mechanism of polymer-based valves and the structure optimization. In the meantime, the performance of other biocompatibility actuation materials, such as polyvinylidene fluoride (PVDF) will be studied, as an alternative material to PZT to drive the micropump.

Acknowledgments This work was partially supported by National Institute of Health (NIH-NIDDK SBIR Phase I Grant R43 DK076320-01A1). The authors also acknowledge the fabrication and characterization assistance at the Nanofabrication Center and the Characterization Facility at the University of Minnesota.

References

Bohm S, Olthuis W, Bergveld P (1999) A plastic micropump constructed with conventional techniques and materials. Sens Actuat A 77:223–228

Chen L, Lee S, Choo J, Lee EK (2008) Continuous dynamic flow micropump for microfluid manipulation. J Micromech Microeng 18:013001 (22 pp)

Cooney CG, Towe BC (2004) A thermopneumatic dispensing micropump. Sens Actuat A 116:519–524

Doll AF, Wischke M, Geipel A, Goldschmidtboeing F, Ruthmann O, Hopt UT, Schrag HJ, Woias P (2007) A novel artificial sphincter prosthesis driven by a four-membrane silicon micropump. Sens Actuat A 139:203–209

Gietzelt T, Piotter V, Reprecht R, Hausselt J (2002) Manufacturing of isolated ceramic microstructures. Microsyst Technol 9:99–103

Han A, Wang O, Graff M, Mohanty SK, Edwards TL, Han KH, Bruno F (2003) A multi-layer plastic/glass microfluidic systems containing electrical and mechanical functionality. Lab chip 3:150–157

Hwang IH, An JY, Ko KH, Shin SM, Lee JH (2007) A novel micropump with fixed-geometry valves and low leakage flow. J Micromech Microeng 17:1632–1639

Kamper KP, Dopper J, Ehrfeld W, Oberbeck S (1998) A self-filling low-cost membrane micropump, In: Proc. IEEE MEMS'98, Heidelberg, Germany (25–29 January, 1998), pp 432–437

Koch M, Harris N, Maas R, Evans AGR, White WM, Brunnschweiler A (1997) A novel micropump design with thick-film piezoelectric actuation. Meas Sci Technol 8:49–57

Lee S, Kim KJ (2006) Design of IPMC actuator-driven valve-less micropump and its flow rate estimation at low reynolds numbers. Smart Mater Struct 15:1103–1109

Lee CY, Chang HT, Wen CY (2008) A MEMS-based valveless impedance pump utilizing electromagnetic actuation. J Micromech Microeng 18:035044 (9 pp)

Nisar A, Afzulpurkar N, Mahaisavariya B, Tuantranont A (2008) MEMS-based micropumps in drug delivery and biomedical applications. Sens Actuat B 130:917–942

Shen M, Yamahata C, Gijs MAM (2008) Miniaturized PMMA ball-valve micropump with cylindrical electromagnetic actuator. Microelectron Eng 85:1104–1107

Truong TQ, Nguyen NT (2004) A polymeric piezoelectric micropump based on lamination technology. J Micromech Microeng 14:632–638

Wego A, Pagel L (2001) A self-filling micropump based on PCB technology. Sens Actuat A 88:220–226

Yoon JS, Choi JW, Lee IH, Kim MS (2007) A valveless micropump for bidirectional applications. Sens Actuat A 135:833–838

Zengerle R, Ulrich J, Kluge S, Richter M, Richter A (1995) A bidirectional silicon micropump. Sens Actuat A 50:81–86